Fusion Group

Barcelona Supercomputing Center
Centro Nacional de Supercomputación

EXCELENCIA SEVERO OCHOA

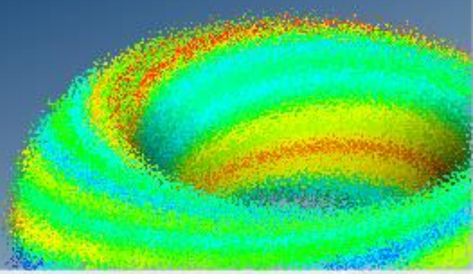

Shear Alfvén wave continuum spectrum with bifurcated helical core equilibria

Allah Rakha

Barcelona Supercomputing Center, Spain

Acknowledgements

Ph.Lauber, Mervi Mantsinen, and D. A. Spong

18th European Fusion Theory Conference
7 – 10 October 2019, Ghent, Belgium

09/10/2019

Gent, Belgium

Outline

Introduction

Experimental findings

Research results

1) Modelling of helical equilibria

2) Modelling of Alfvén continua with helical core for AUG

Summary

Future work

3D effects in tokamaks

Toroidal field coils

External 3D

Resonant magnetic perturbation coils

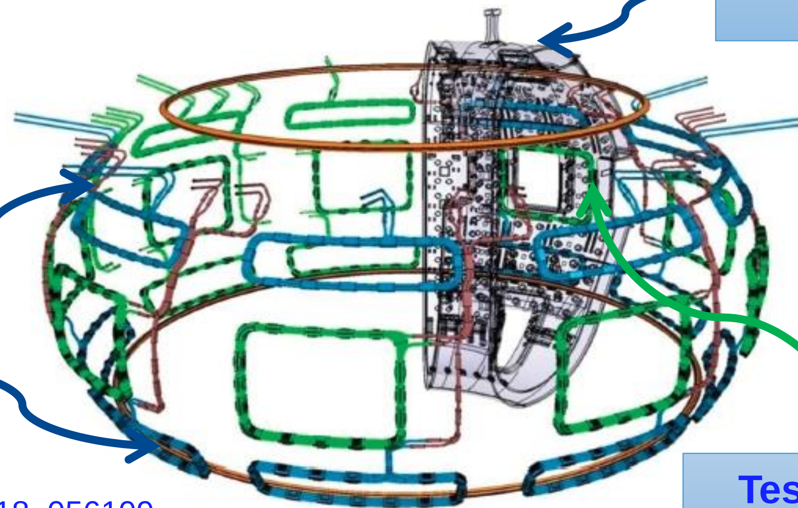

Test blanket module

D A Spong Phys. Plasmas 18, 056109 (2011)

Internal 3D

Helical core

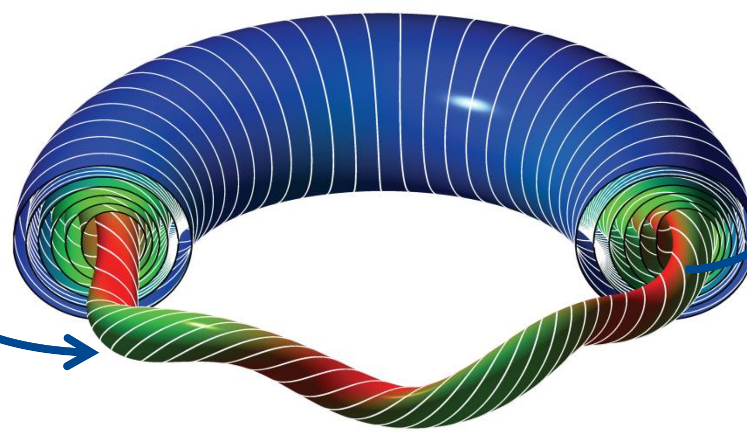

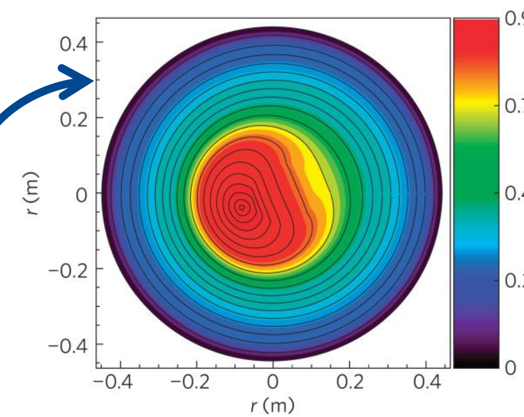

A. Wingen 2016 ORNL

Barcelona Supercomputing Center
Centro Nacional de Supercomputación

Observation of BAEs during sawtooth cycles

- Experimentally **low-frequency** beta induced Alfvén eigenmodes (BAEs), which are **long-lived modes (LLM)** have been observed during monster sawtooth cycles.
- They are predicted with extended regions of low or reversed-shear profiles having rational surfaces of (q ≈ 1).
- Observation of LLMs is associated with the presence of 3D helical core. Chapman et al. Nucl. Fusion 50 045007, 2010

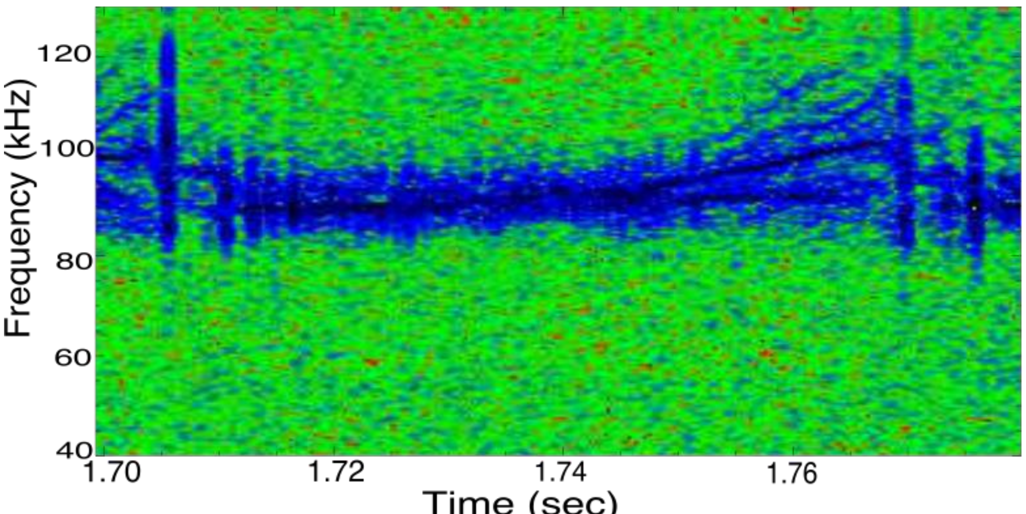

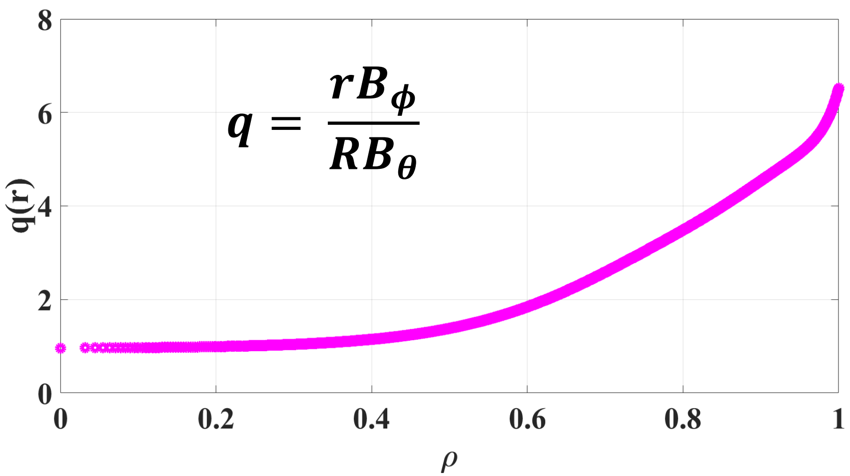

Allah Rakha et al. Nucl. Fusion 59 106042, 2019

Numerical tools and flow chart

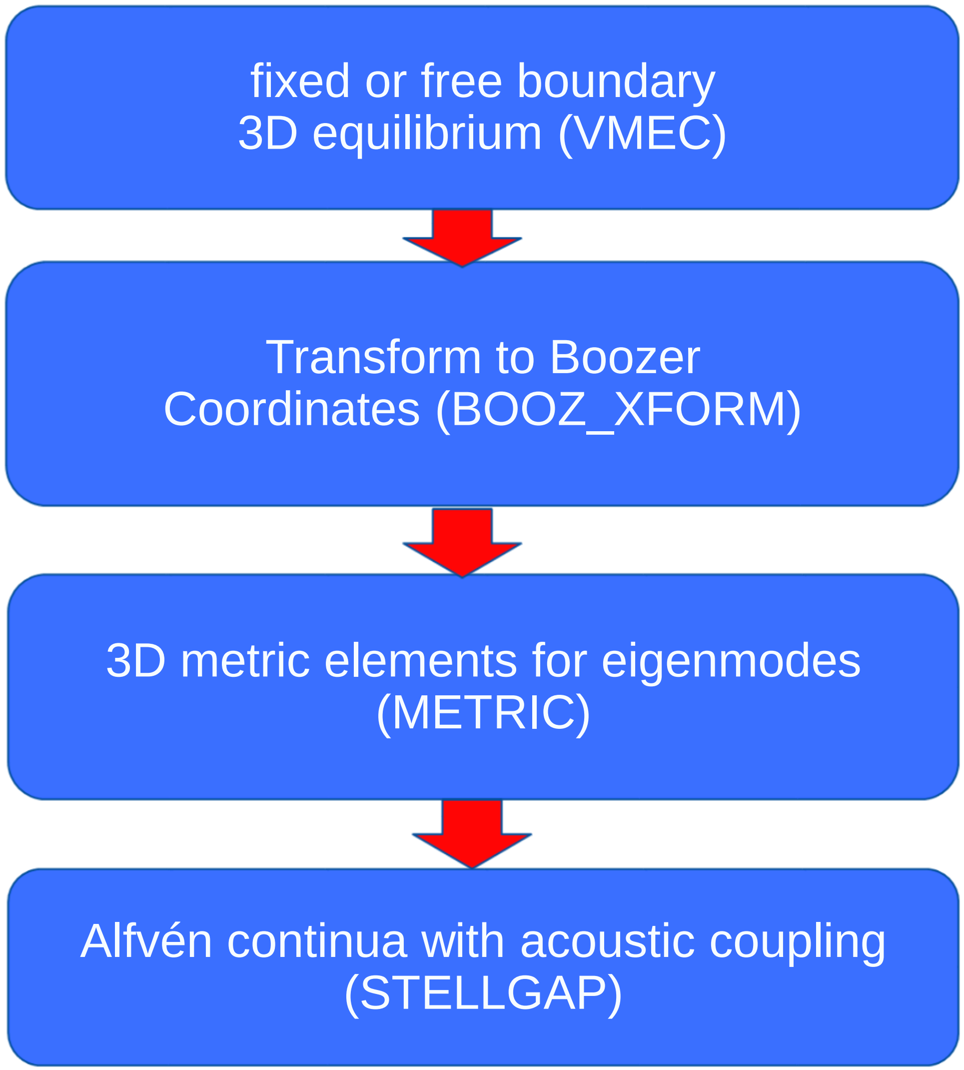

D.A. Spong, Phys. Plasmas 17 (2010) 022106

Modelling tool (STELLGAP)

STELLGAP computes **continuum structure** of shear Alfvén waves and the **gaps** which appear on the counter propagation of shear Alfvén waves in wide range of 3D fusion devices.

Alfvén continuum equation for 3D equilibria in the compressible limit;

$$\left(\mu_0\rho_m\omega^2\frac{|\vec{\nabla}\psi|^2}{B^2} + \vec{B}\cdot\vec{\nabla}\left[\frac{|\vec{\nabla}\psi|^2(\vec{B}\cdot\vec{\nabla})}{B^2}\right]\right)\xi_s + \gamma p K_s(\vec{\nabla}\cdot\vec{\xi}) = 0$$

$$K_s\xi_s + \left[\frac{\gamma p + B^2}{B^2} + \frac{1}{\mu_0\rho_m\omega^2}\gamma p(\vec{B}\cdot\vec{\nabla})\frac{(\vec{B}\cdot\vec{\nabla})}{B^2}\right](\vec{\nabla}\cdot\vec{\xi}) = 0$$

Incompressible STELLGAP

Inertia energy

bending

Plasma Compressibility

D.A. Spong, Phys. Plasmas 10 (2003) 3217

Modelling tool (STELLGAP)

$$\left(\mu_0\rho_m\omega^2\frac{|\vec{\nabla}\psi|^2}{B^2}+\vec{B}\cdot\vec{\nabla}\left[\frac{|\vec{\nabla}\psi|^2(\vec{B}\cdot\vec{\nabla})}{B^2}\right]\right)\xi_s+\gamma p K_s(\vec{\nabla}\cdot\vec{\xi})=0$$

Inertia energy **bending**

$$K_s\xi_s+\left[\frac{\gamma p+B^2}{B^2}+\frac{1}{\mu_0\rho_m\omega^2}\gamma p(\vec{B}\cdot\vec{\nabla})\frac{(\vec{B}\cdot\vec{\nabla})}{B^2}\right](\vec{\nabla}\cdot\vec{\xi})=0$$

Geodesic curvature

$$K_s=2\vec{\kappa}\cdot\left(\vec{B}\times\frac{\vec{\nabla}\psi}{B^2}\right)\text{ with }\quad\vec{\kappa}=\left(\vec{b}\cdot\vec{\nabla}\right)\vec{b}\quad\text{and}\quad\vec{b}=\frac{\vec{B}}{B}$$

Using parallel gradient $\mathbf{B}\cdot\nabla=\frac{1}{\sqrt{g}}\left(\iota\frac{\partial}{\partial\theta}+\frac{\partial}{\partial\zeta}\right)$ and $|\nabla\psi|^2=g^{\rho\rho}\left(\frac{d\psi}{d\rho}\right)^2$ operators, eigenvalue system.

$$\omega^2\overleftrightarrow{A}\mathbf{x}=\overleftrightarrow{B}\mathbf{x}\qquad\mathbf{x}=[E_\psi^1\ E_\psi^2\ E_\psi^3\ \cdots\ E_\psi^L]^T.$$

Research results (Part-I)

Modelling of helical equilibria

Axisymmetric (2D) MHD equilibria

In AUG tokamak plasma (20488) axisymmetric MHD equilibrium has been reconstructed with experimental pressure and q-profile.

$\phi = 0 \;\&\; \pi/2$

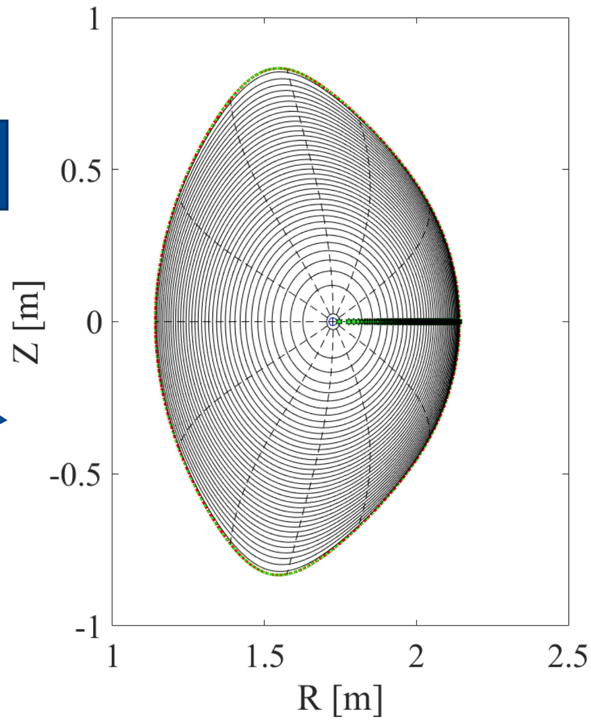

$\phi = \pi/2 \;\&\; \pi$

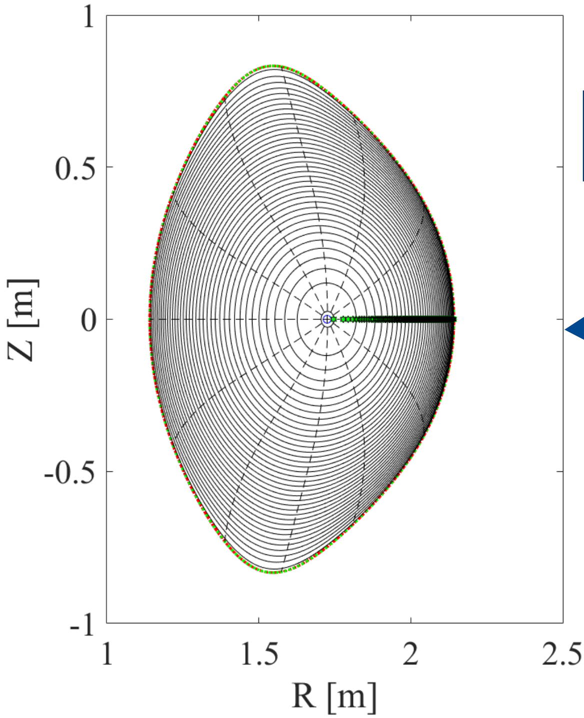

The concentric and regular flux-surfaces without any excursion of the magnetic axis are the evidence of its axisymmetric calculation.

Allah Rakha et al. Nucl. Fusion 59 106042, 2019

Bifurcated helical core MHD equilibria

In AUG tokamak plasma (20488) bifurcated helical core MHD equilibrium has been reconstructed with experimental pressure and q-profile by adding a seed perturbation in magnetic axis.

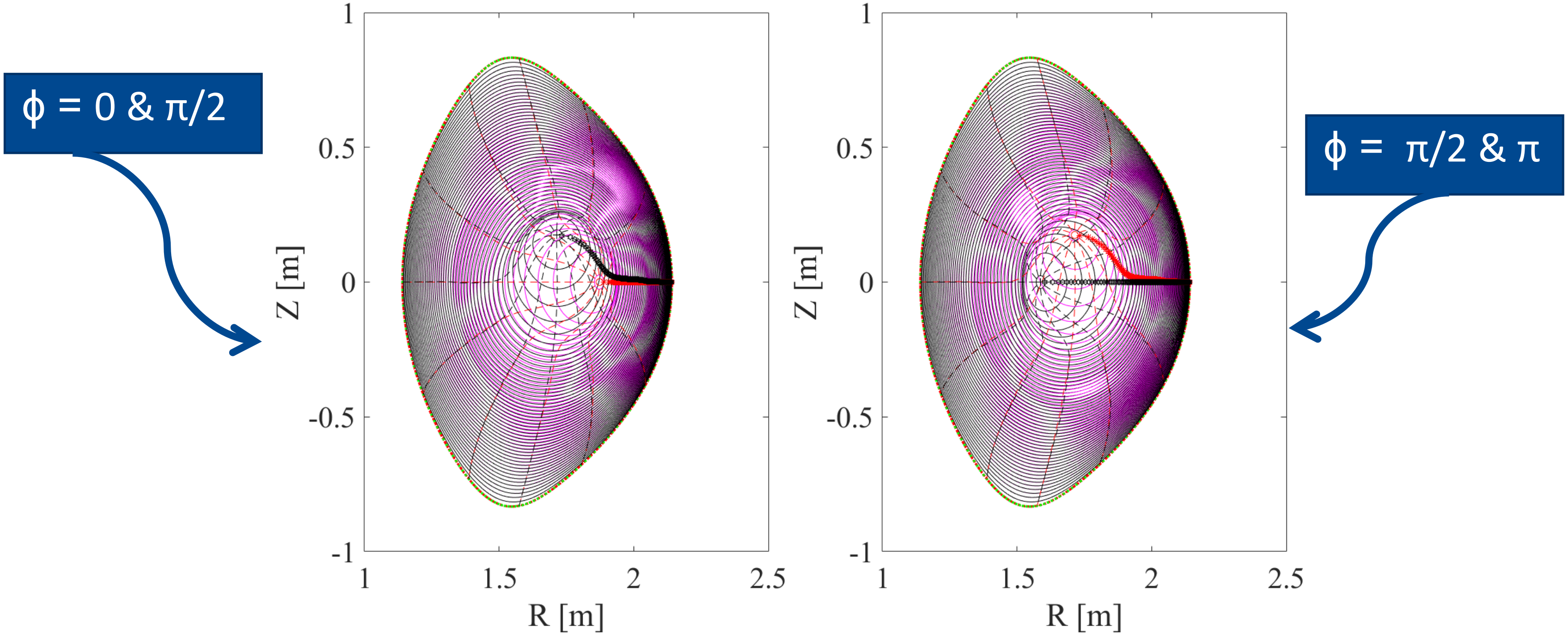

The irregular flux-surfaces with clear excursion of the magnetic axis are the evidence of its non-axisymmetric calculations.

Barcelona Supercomputing Center
Centro Nacional de Supercomputación

Allah Rakha et al. Nucl. Fusion 59 106042, 2019

Helical core excursion with pressure

Equilibrium reconstruction with the pressure scaling show an increase in the helical excursion of the magnetic axis (helical core)

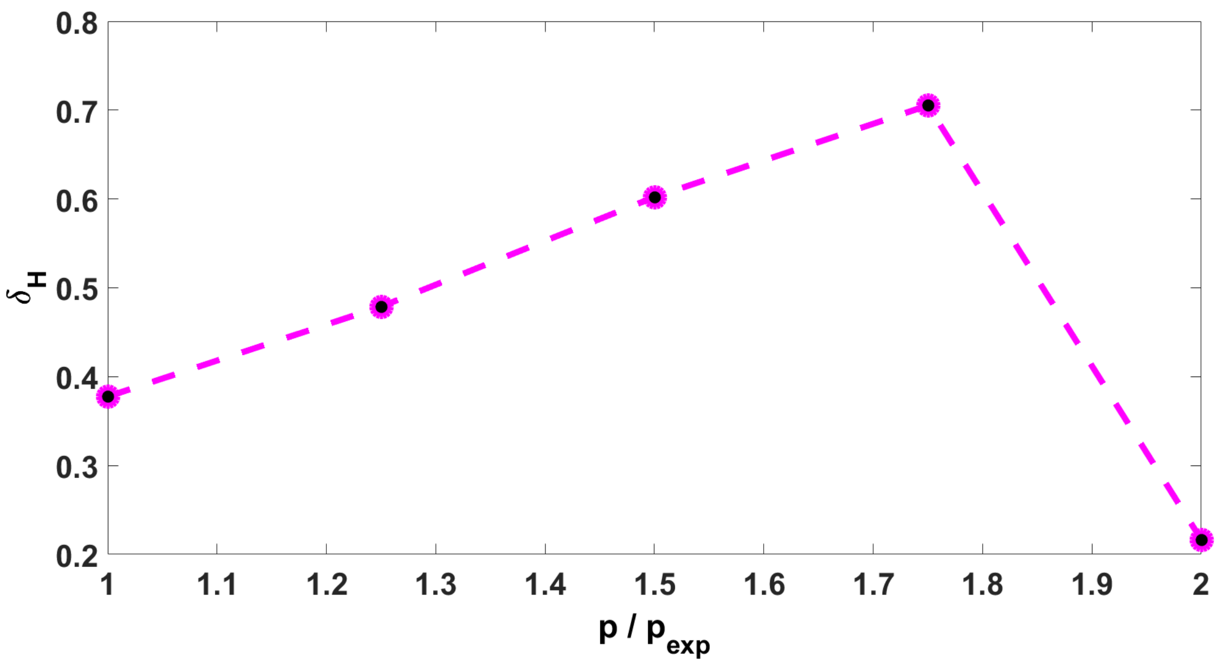

Decrease in the helical excursion δ_H happens in the **fixed boundary** MHD equilibrium calculations.

At peaked pressure, **Shafranov shift** already distorts enough magnetic flux surfaces and leaves no room for their further stretching.

Allah Rakha et al. Nucl. Fusion 59 106042, 2019

Research results (Part-II)

Modelling of Alfvén continua with helical core for the AUG plasmas

fusion group

Alfvén continuum structures with Axisymmetric MHD equilibria & p/p_{exp}=1

Alfvén continuum structures computed with 2D MHD equilibrium do not show any splitting in Alfvén continua around the frequency accumulation point (FAP).

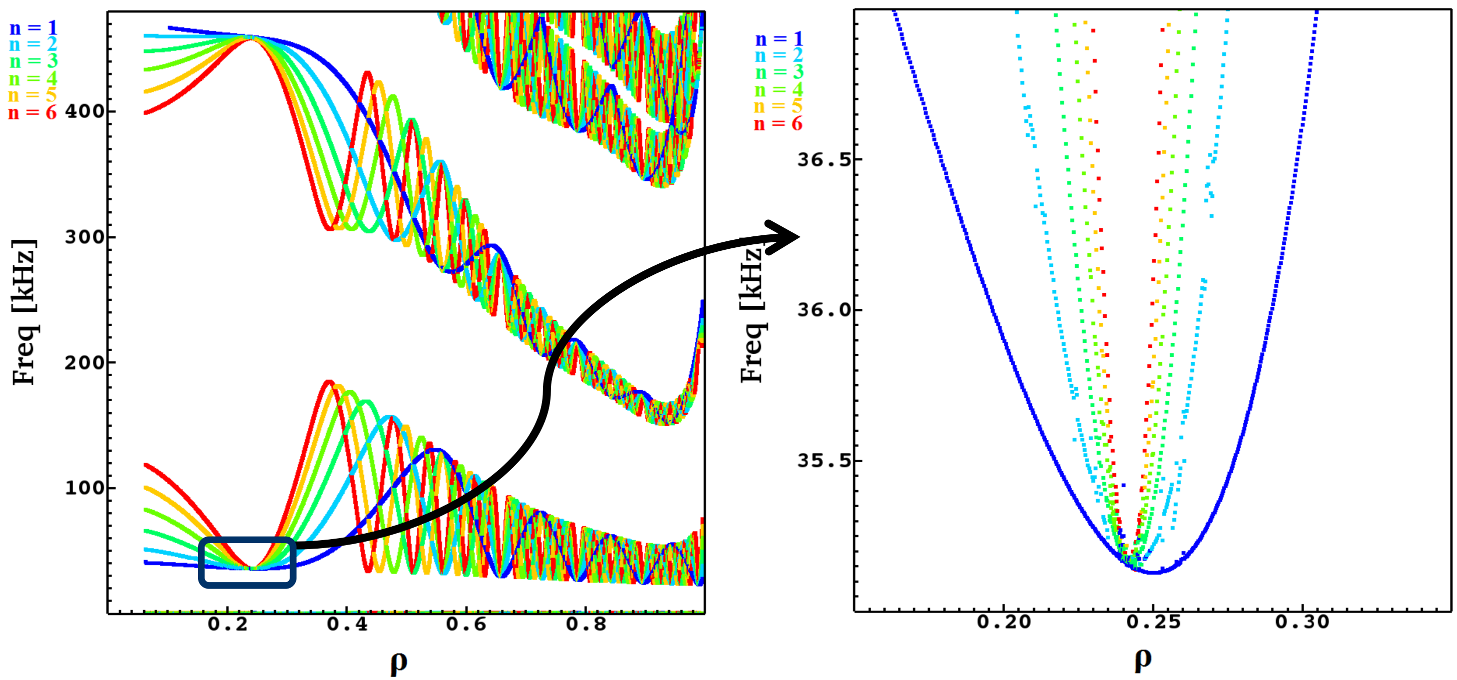

Allah Rakha et al. Nucl. Fusion 59 106042, 2019

Alfvén continua with 3D helical core equilibria & $p/p_{exp}=1$

Alfvén continuum structures computed with 3D helical core MHD equilibrium show frequency splitting in Alfvén continua around the frequency accumulation point (FAP).

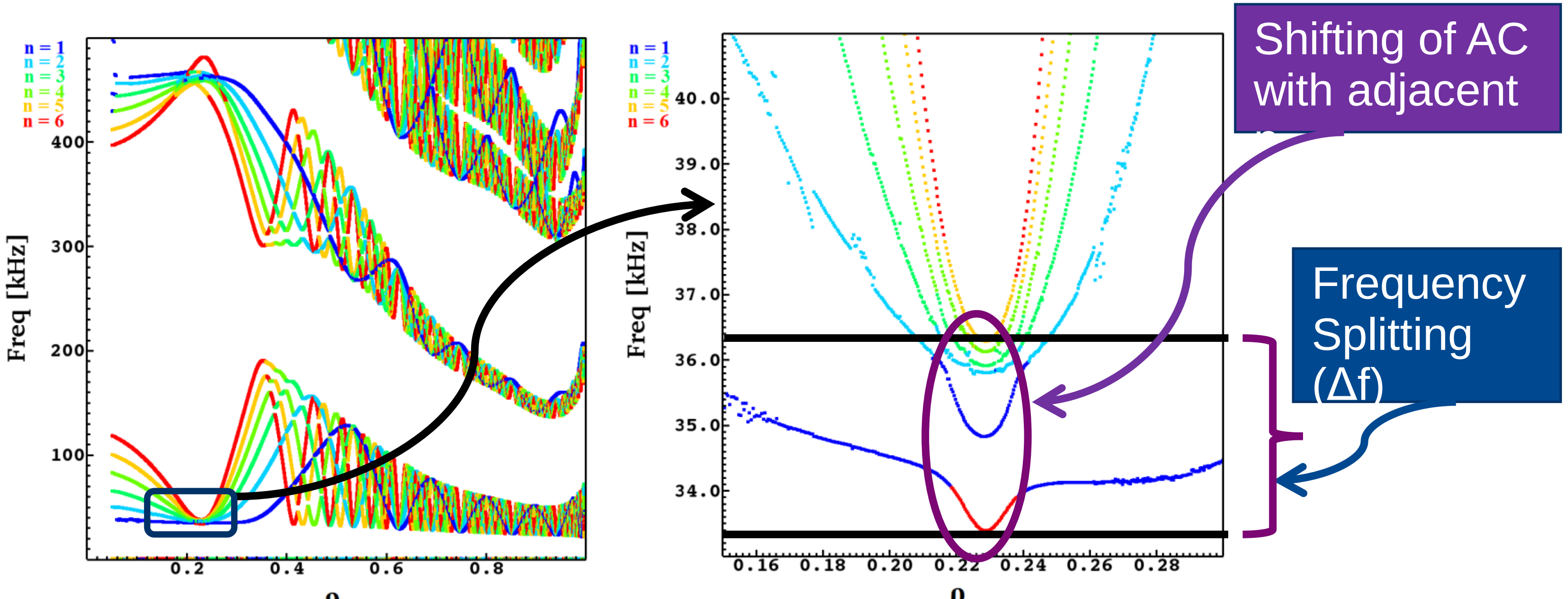

Splitting in AC frequency around the FAP appears due to 3D helical perturbation of magnetic axis.

Allah Rakha et al. Nucl. Fusion 59 106042, 2019

Alfvén continua with 3D helical core equilibria & p/p_{exp}=1.75

Alfvén continuum structures computed with 3D helical core and higher plasma pressure **enhance frequency splitting** in Alfvén continua around the (FAP).

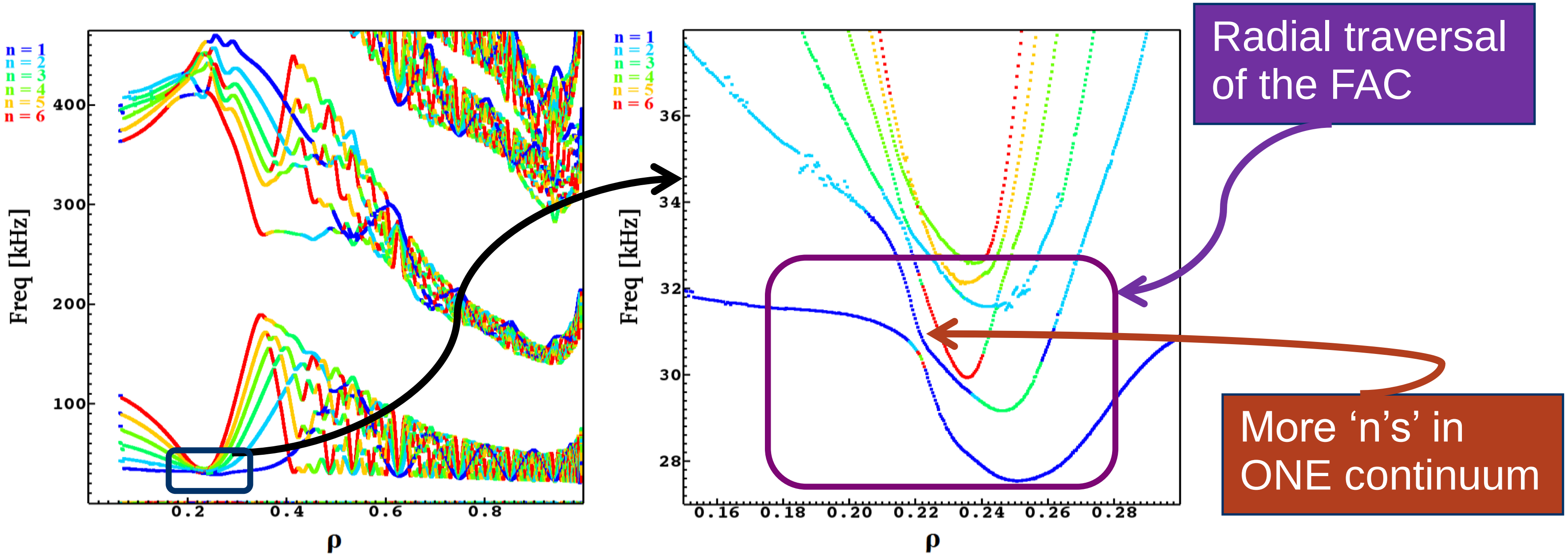

Allah Rakha et al. Nucl. Fusion 59 106042, 2019

Alfvén continuum frequency splitting with helical excursion

Frequency splitting (Δf) (difference between the maximum and the minimum frequency branches of AC around FAP) increases with δ_H up to 5 kHz.

The increase in Δf with δ_H explains remaining differences of few kHz of kinetic calculations with diamagnetic frequency (ω*) (Ph.Lauber)

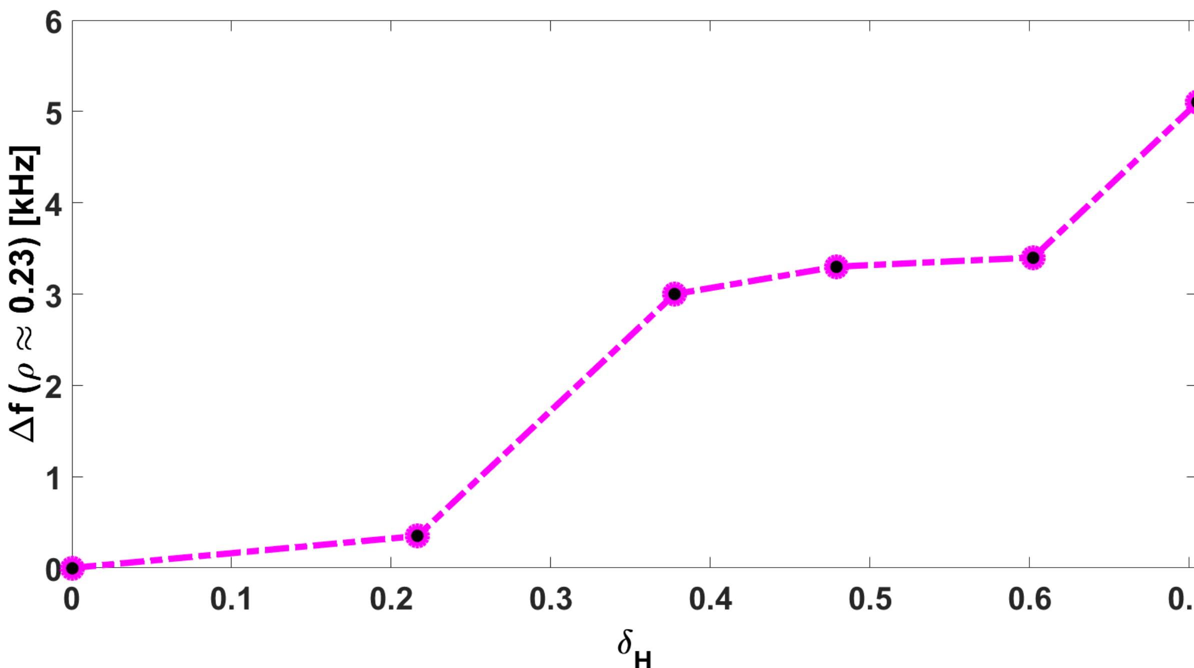

Ph. Lauber et al 2009 PPCF 51 124009

D. Curran et al 2012 PPPCF 54 055001

Allah Rakha et al. Nucl. Fusion 59 106042, 2019

Generation of helical gaps for HAE

Radial variation (distortion) in Alfvén continuum structures generates helical gaps to accommodate helical Alfvén modes (HAE) of multiple n,m.

Zero-helical excursion ($\delta_H = 0$)

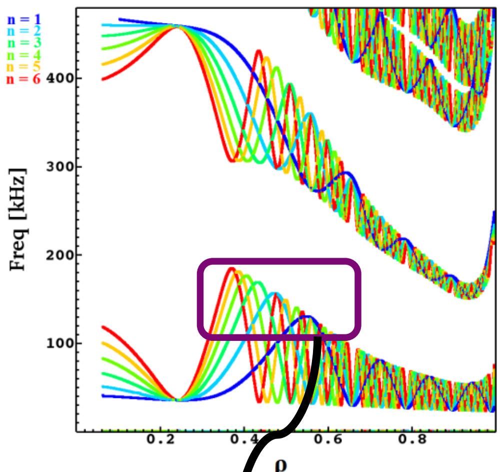

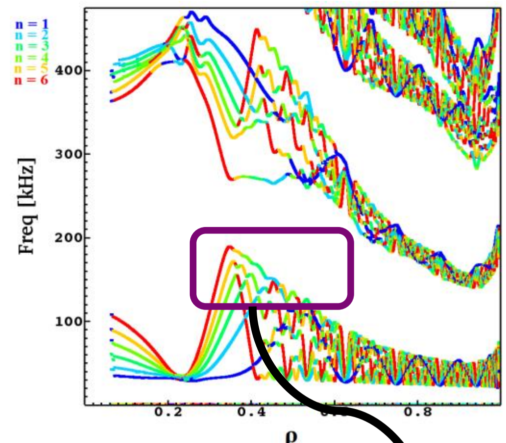

Max-helical excursion ($\delta_H = 0.7$)

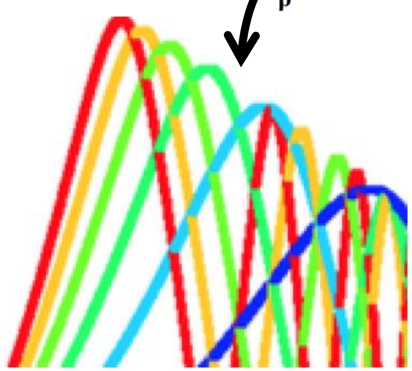

Helical gaps

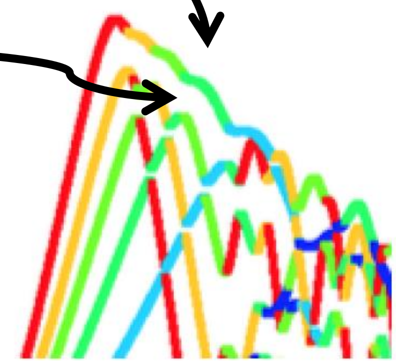

Allah Rakha et al. Nucl. Fusion 59 106042, 2019

Radial variation (distortion) in Alfvén continuum with helical excursion

- Radial variation (distortion) in the computed continuum structures increases with δ_H.
- Helical excursion not only splits the AC in frequency range it also distorts them along the radial extent.

It generates new gaps in Alfvén continua called helical gaps (HAEs).

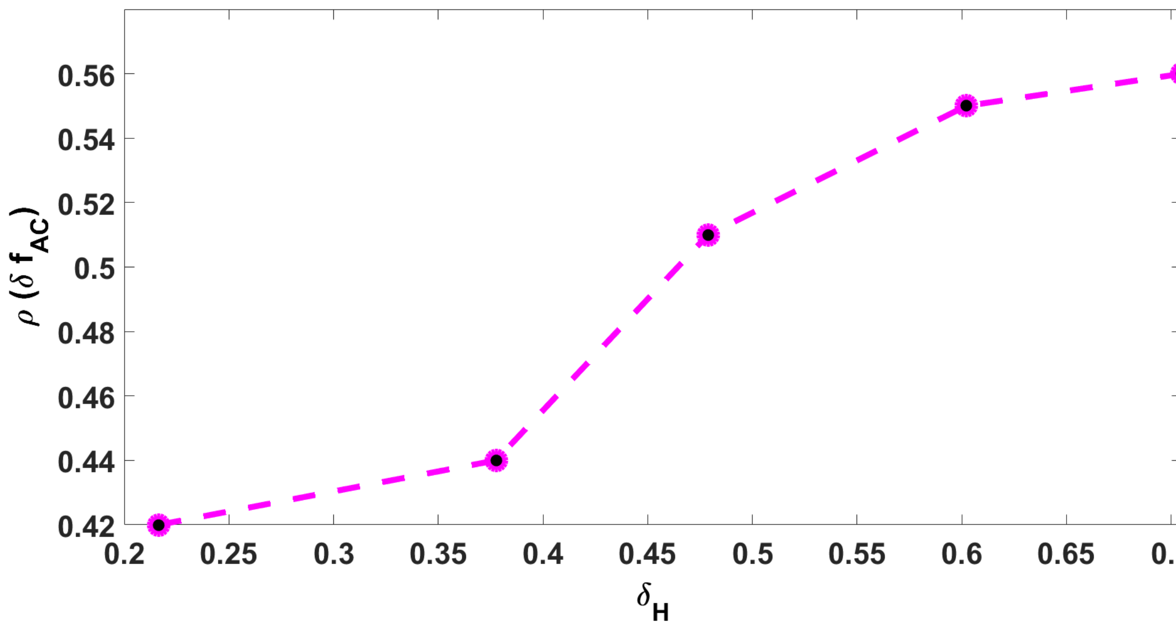

Allah Rakha et al. Nucl. Fusion 59 106042, 2019

Summary and outlook

Summary of results

- Reconstruction of bifurcated helical core MHD equilibria using VMEC code in fixed-boundary approximation for AUG plasmas with q ≈ 1.
- Remaining differences with kinetic simulations of frequency splitting at FAP of AC structures are explained with 3D helical core equilibria.
- Shifting of AC with adjacent ‘n’ has been determined around the FAP.
- HAE gaps in AC structures with 3D helical core equilibria are found.

Future work

- Reconstruction of bifurcated helical core MHD equilibria with free-boundary calculations and its impact on the AC structures.
- Modelling of HAEs properties (mode numbers (m, n), frequency, radial localization and growth rate) expected in these helical gaps.
- Helical core MHD equilibrium reconstruction with magnetic islands and stochastic regions using SIESTA, PIES, or HINT codes instead of VMEC and its effect on Alfvén continua and modes.

Fusion Group

Barcelona Supercomputing Center
Centro Nacional de Supercomputación

EXCELENCIA SEVERO OCHOA

Acknowledgements

Generalitat de Catalunya

AGAUR

FUSENET

Thank you

EUROfusion

allah.rakha@bsc.es

(Back-up)

fusion group

Motivation: Observation of Long-lived modes (LLM)

- Long Lived Modes resemble with (n=m=1) saturated helical mode.
- As q_{min} approaches unity, LLM appears and fast ions are expelled from plasma core. M. Garcia-Munoz et.al, PRL 100,055005 (2008)

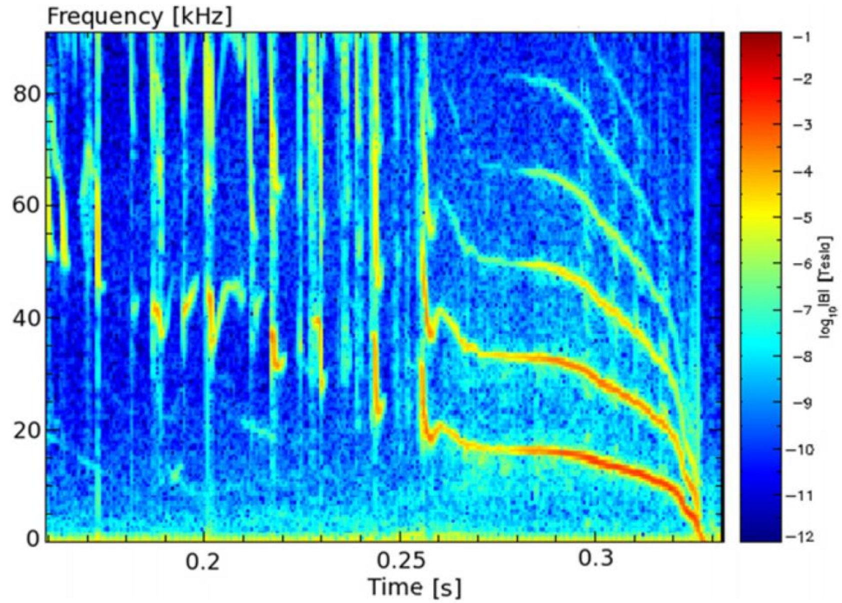

Chapman et al 2010 Nucl. Fusion 50 045007

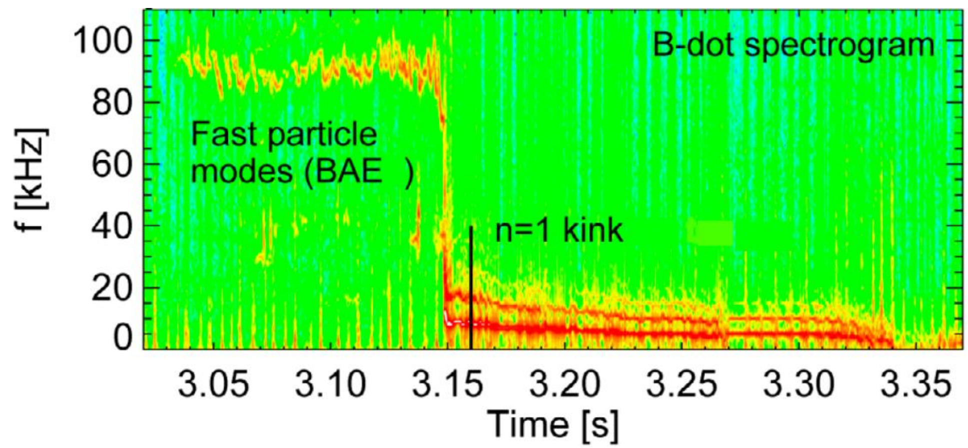

AUG 32456, Observation of n = 1 saturated internal-kind-modes.

P Piovesan et al. PPCF 59 (2017) 014027

Motivation: Kinetic theory description

kinetic BAE dispersion relation [Zonca NF 2009, Lauber PPCF 2009] predicts splitting of modes with different mode numbers at q=1 surface (m=n)

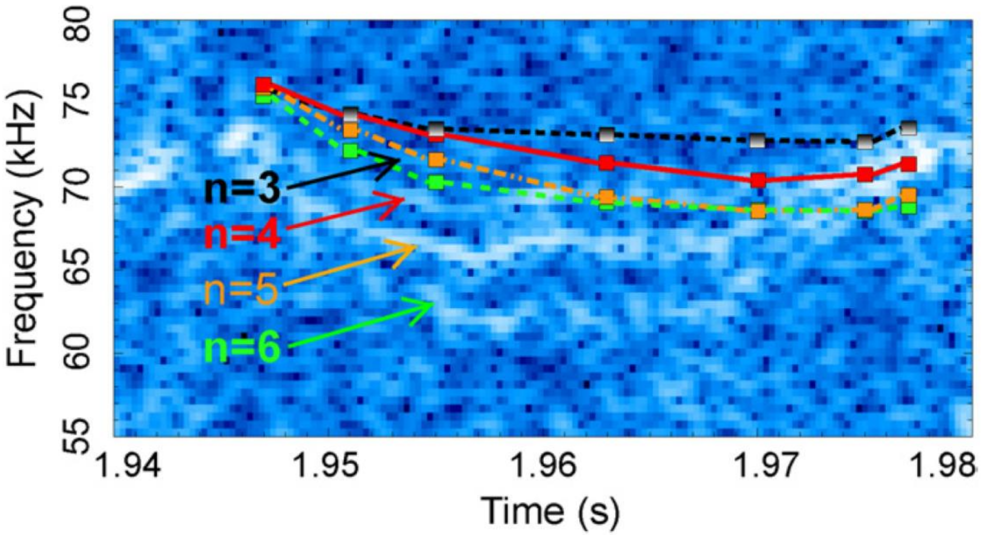

D Curran et al 2012 PPCF 54 055001

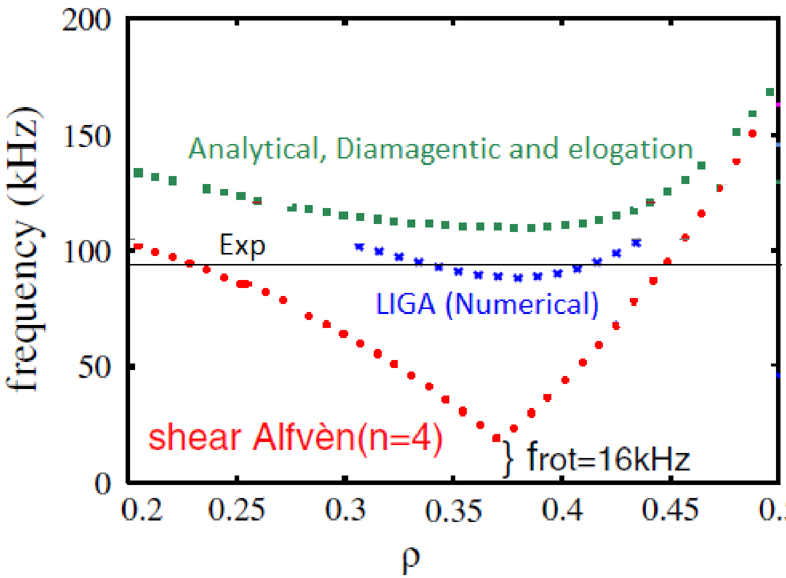

Ph Lauber et al 2009 PPCF 51 124009

Kinetic calculation including diamagnetic drift (ω*) could not explain the differences of frequencies around the accumulation point.

Motivation: Observation of Long-lived modes (LLM)

- Long Lived Modes resemble with (n=m=1) saturated helical modes.
- As q_{min} approaches unity, LLM appears and can radially transport fast ions. M. Garcia-Munoz et.al, PRL 100,055005 (2008)

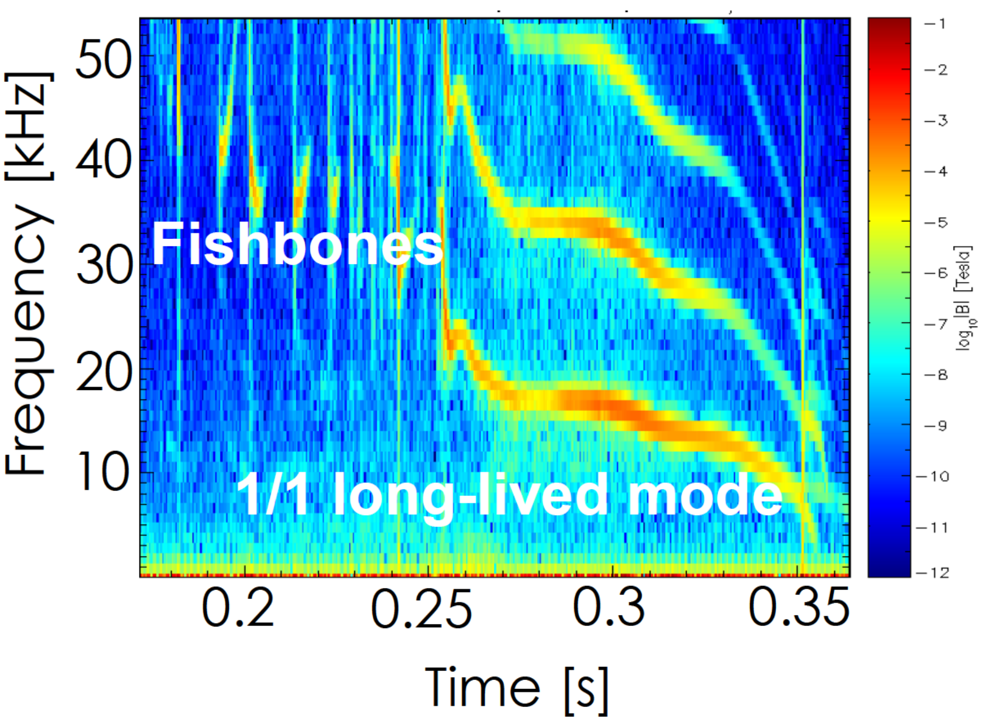

Chapman et al. Nucl. Fusion 50 045007, 2010

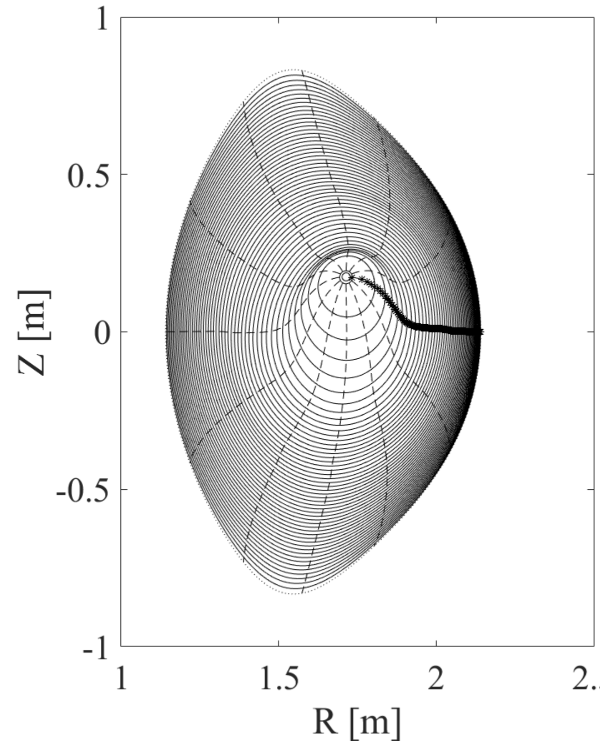

Allah Rakha et al. Nucl. Fusion 59 106042, 2019

3D effects in tokamaks

Toroidal field coils: mostly high-n perturbations, e.g. n=16 in AUG

Test blanket modules: low-n perturbation (n=1) in ITER

RMP coils: low-n perturbations, e.g. n=1, 2 or 4 in AUG

resistive wall: medium-n perturbation (n=9) in ITER

error fields: small undesignedly or unavoidable non-axisymmetric magnetic fields $(\Delta B/B) \sim 10^{-4}$

External 3D

equilibrium with helical core: low-n perturbation, observed in MAST, TCV, RFX, ….

Internal 3D

n= leading toroidal harmonic of the magn. field perturbation

ASDEX Upgrade tokamak

- **ASDEX Upgrade** (**A**xially **S**ymmetric **D**ivertor **Ex**periment) is a Medium size divertor tokamak, at the Max-Planck-Institut für Plasmaphysik, Garching .
- It is the Germany's second largest fusion experiment after stellarator Wendelstein 7X.

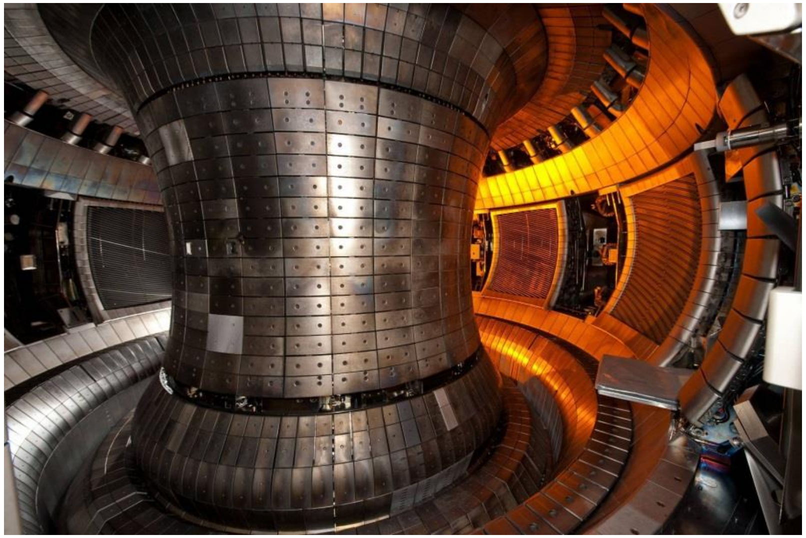

ASDEX Upgrade parameters	
Major plasma radius (R)	1.6 m
Minor plasma radius (a)	0.5/0.8 m
Magnetic field (B)	3.9 T
Plasma Current (Ip)	2 MA
Pulse length	10 s
Plasma heating	27 MW
Plasma mixture	H, D
Plasma density (n_e)	2×10^{20} / m^3
Plasma temperature (T)	100 MK
Plasma quantity	3 mg
Plasma volume	13 m^3
Total height of device	9 m

Barcelona Supercomputing Center
Centro Nacional de Supercomputación

Convergence of helical core equilibria

Convergence of the helical core equilibrium has been achieved by computing the residual force balance, the gradual decrease of <FR> with Nit confirms it.

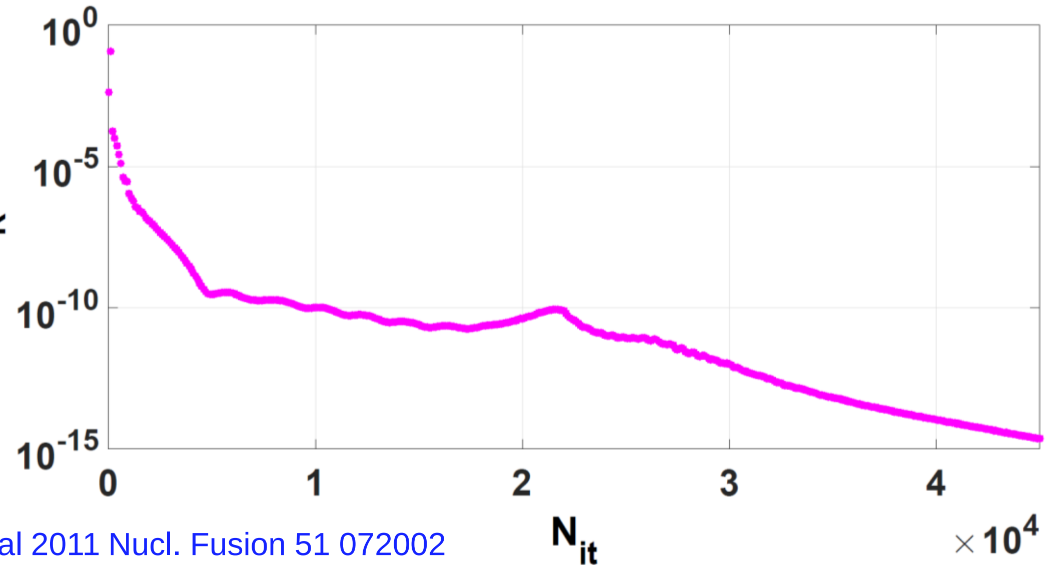

W.A. Cooper et al 2011 Nucl. Fusion 51 072002

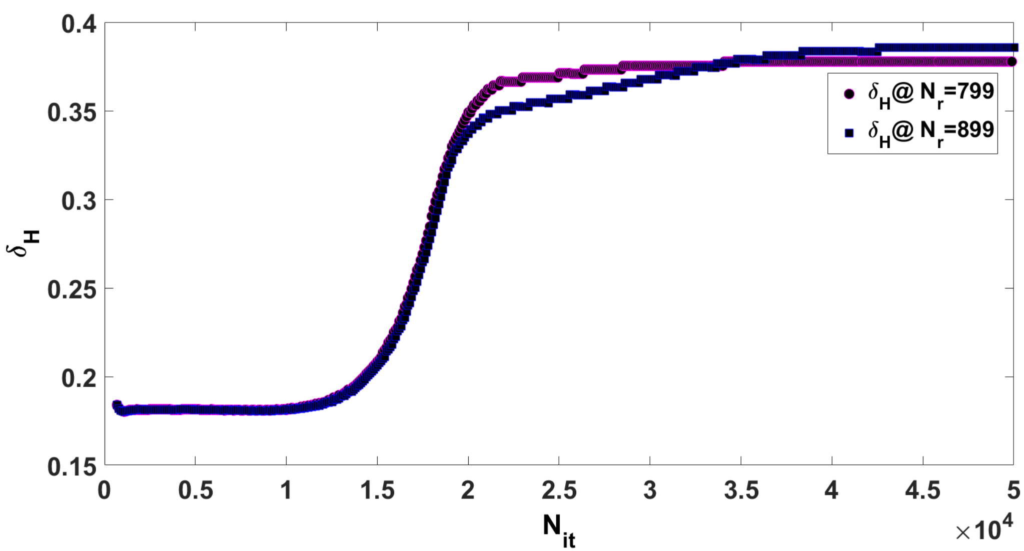

Saturation of the helical excursion of magnetic axis with Nit also confirms the convergence of our results

A. Wingen et al 2018 Nucl. Fusion 58 036004

Variation of Alfvén continuum gaps with the helical excursion

Three major gaps are found at three different radial locations in all three computed continua.

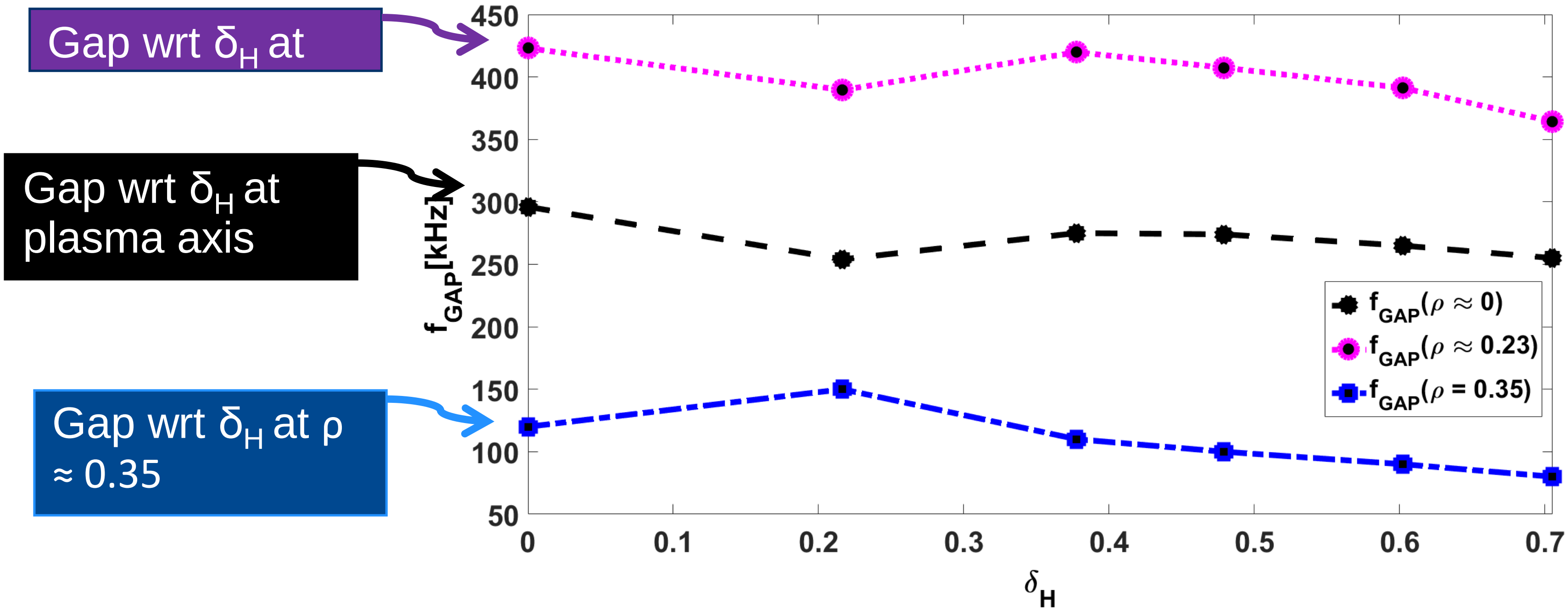

Radial variation of FAP after frequency splitting in AC structures with δ_H

Radial variation of the FAP with δ_H shows that maximum and minimum frequency branches of the AC remain consistent with δ_H. Only there is small variation of 0.14 at $\delta_H = 0.7$

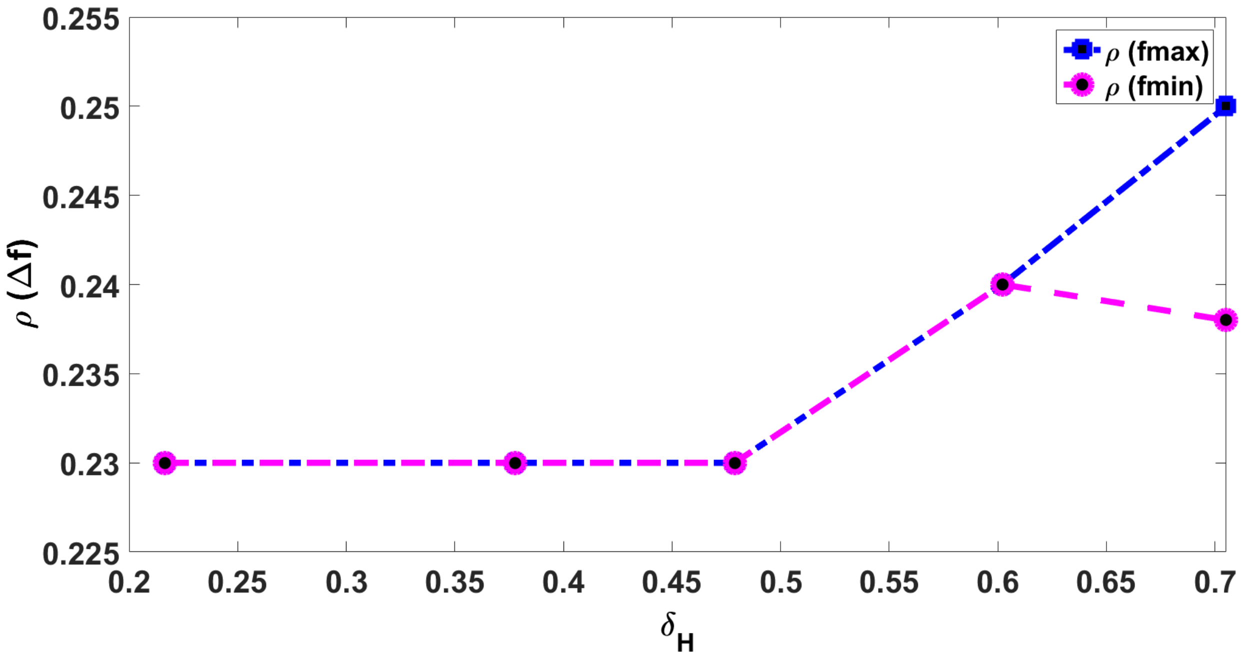

Allah Rakha et al. Nucl. Fusion 59 106042, 2019

Summary and outlook

- Reconstruction of bifurcated helical core MHD equilibria using fixed-boundary for ASDEX Upgrade plasmas with q ≈ 1.
- Due to 3D helical core, frequency splitting in the AC structures around the FAP is determined. Remaining differences of kinetic simulations are explained with 3D helical core structures.
- Shifting of AC with adjacent ‘n’ has been determined around the FAP.
- Radially FAP remains fixed for lower helical excursion (δ_H) and with higher δ_H it radially shifts slightly.
- Additional frequency gaps in AC structures are determined called HAE gaps, appear due to 3D helical excursion of the magnetic axis.

- Reconstruction of bifurcated helical core MHD equilibria with free-boundary calculations and its impact on the AC structures.
- Modelling of HAEs properties (mode numbers (m, n), frequency, radial localization and growth rate) expected in these helical gaps

Helical distortion during sawtooth cycles

Internal Kink Mode

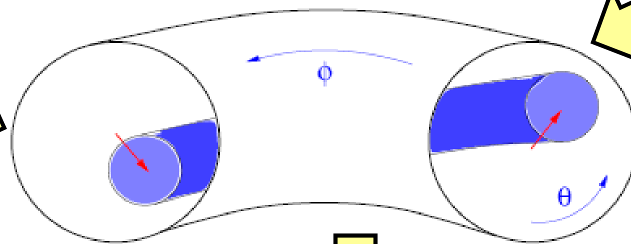

Destabilise kink mode

Drive current near mode location or introduce fast ions just outside mode location

Saturation of internal kink-like mode leads to helical core formation

Sawtooth Oscillations

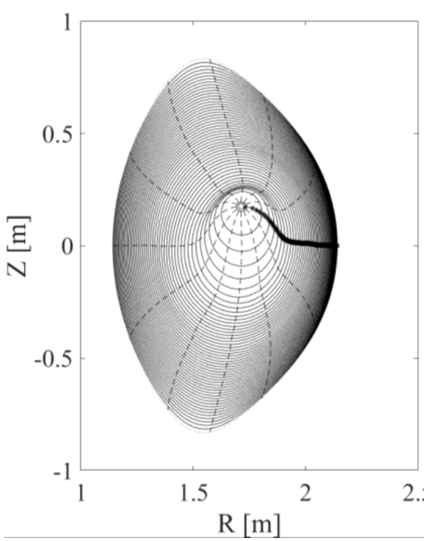

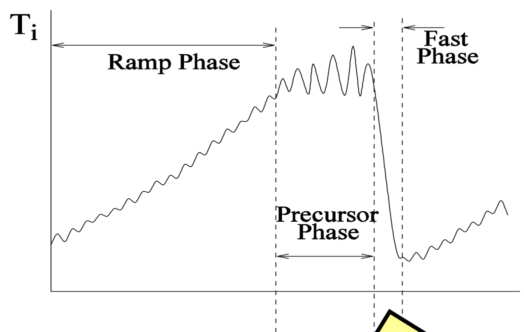

Long Sawteeth

With steep ∇p

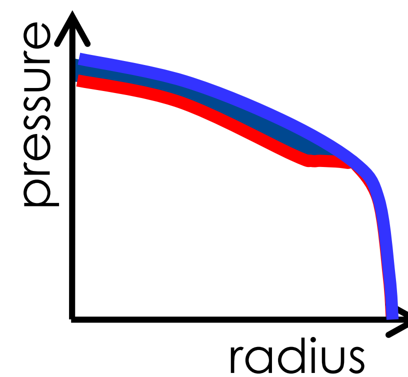

Modelling tool (STELLGAP)

STELLGAP computes **continuum structure** of shear Alfvén waves and the **gaps** which appear on the counter propagation of shear Alfvén waves in wide range of 3D fusion devices.

Alfvén continuum equation for 3D equilibria in compressible limit is;

Incompressible STELLGAP

$$\left(\mu_0\rho_m\omega^2\frac{|\vec{\nabla}\psi|^2}{B^2}+\vec{B}\cdot\vec{\nabla}\left[\frac{|\vec{\nabla}\psi|^2(\vec{B}\cdot\vec{\nabla})}{B^2}\right]\right)\xi_s+\gamma p K_s(\vec{\nabla}\cdot\vec{\xi})=0$$

Inertia energy — bending

Plasma Compressibility

$$K_s\xi_s+\left[\frac{\gamma p+B^2}{B^2}+\frac{1}{\mu_0\rho_m\omega^2}\gamma p(\vec{B}\cdot\vec{\nabla})\frac{(\vec{B}\cdot\vec{\nabla})}{B^2}\right](\vec{\nabla}\cdot\vec{\xi})=0$$

Geodesic curvature

$$K_s=2\vec{\kappa}\cdot\left(\vec{B}\times\frac{\vec{\nabla}\psi}{B^2}\right)\ \text{with}\quad \vec{\kappa}=\left(\vec{b}\cdot\vec{\nabla}\right)\vec{b}\quad\text{and}\quad \vec{b}=\frac{\vec{B}}{B}$$

Using parallel gradient $\mathbf{B}\cdot\nabla=\frac{1}{\sqrt{g}}\left(\iota\frac{\partial}{\partial\theta}+\frac{\partial}{\partial\zeta}\right)$ and $|\nabla\psi|^2=g^{\rho\rho}\left(\frac{d\psi}{d\rho}\right)^2$ operators, eigenvalue system.

$$\omega^2\overleftrightarrow{A}\mathbf{x}=\overleftrightarrow{B}\mathbf{x}\qquad \mathbf{x}=[E_\psi^1\ E_\psi^2\ E_\psi^3\ \cdots\ E_\psi^L]^T.$$